



Sea ice-related halogen enrichment at Law Dome, coastal East Antarctica

Paul Vallelonga^{1*}, Niccolo Maffezzoli¹, Andrew D. Moy^{2,3}, Mark A.J. Curran^{2,3}, Tessa R. Vance³, Ross Edwards⁴, Gwyn Hughes⁴, Emily Barker⁴, Gunnar Spreen⁵, Alfonso Saiz-Lopez⁶, J. Pablo Corella⁶,
5 Carlos A. Cuevas⁶ and Andrea Spolaor^{7,8}

¹Centre for Ice and Climate, Niels Bohr Institute, University of Copenhagen, Juliane Maries Vej 30, Copenhagen Ø 2100 Denmark.

²Australian Antarctic Division, Channel Highway, Kingston, Tasmania 7050, Australia.

³Antarctic Climate and Ecosystem Cooperative Research Centre, University of Tasmania, Private Bag 80, Hobart, Tasmania
10 7001, Australia.

⁴Physics and Astronomy, Curtin University of Technology, Kent St, Bentley WA 6102, Australia.

⁵University of Bremen, Institute of Environmental Physics, Otto-Hahn-Allee 1, 28359 Bremen, Germany.

⁶Department of Atmospheric Chemistry and Climate, Institute of Physical Chemistry Rocasolano, CSIC, Serrano 119, 28006 Madrid, Spain

⁷Ca'Foscari University of Venice, Department of Environmental Sciences, Informatics and Statistics, Via Torino 155, 30170 Venice Mestre, Italy.

⁸Institute for the Dynamics of Environmental Processes, IDPA-CNR, Via Torino 155, 30170 Venice Mestre, Italy.

Correspondence to: Paul Vallelonga (vallelonga@nbi.ku.dk)

20 **Abstract.** The Law Dome site is ideal for the evaluation of sea ice proxies due to its location near to the Antarctic coast, regular and high accumulation throughout the year, an absence of surface melting or remobilization, and minimal multiyear sea ice. We present records of bromine and iodine concentrations and their enrichment beyond seawater compositions, arguing that halogen enrichment is indicative of the local sea ice area, particularly the 90-110° E sector of the Wilkes coast. Our findings support the results of previous studies of sea ice variability from Law Dome, indicating that Wilkes coast sea
25 ice area is currently at its lowest level since the start of the 20th century. From the Law Dome DSS1213 firn core, 26 years of monthly deposition data indicate that the period of peak bromine enrichment is during Austral spring-summer, from November to February. Results from a traverse along the lee (Western) side of Law Dome show low levels of sodium and bromine deposition, with the greatest fluxes in the vicinity of the Law Dome summit. Finally, iodine enrichment is well correlated to that of bromine, indicating a common, sea ice source for their enrichment.

30

Keywords. Antarctica, Halogens, Bromine, Iodine, Law Dome, sea ice, sea ice reconstruction, polar halogen chemistry



1 Introduction

The occurrence of enhanced concentrations of bromine in the boundary-layer above seasonal Antarctic sea ice has been linked to the depletion of tropospheric ozone and mercury (Simpson et al., 2015). Tropospheric ozone is critical to solar forcing, UV absorption and aerosol formation in the polar regions whereas the concentration of mercury in polar snow is a matter of great concern for Arctic ecosystems in the future (Brooks et al., 2006; Hylander and Goodsite, 2006). Recent studies indicate that boundary layer bromine is driven by photochemical recycling above the salt-rich snow and ice surfaces, with such recycling predominantly occurring in the Austral spring, when the concentration of surface salts and surface area of first-year sea ice are at their greatest (Pratt et al., 2013; Zhao et al., 2016). Winter sources of bromine emissions have also been observed although the relative influence of such sources is still a topic of investigation (Impey et al., 1997; Nerentorp Mastromonaco et al., 2016; Simpson et al., 2007).

Reactive iodine has a global influence on ozone depletion and the oxidizing capacity of the polar atmosphere by influencing the repartitioning of HO_x and NO_x (Saiz-Lopez et al., 2012). In particular, large amounts of oxidized iodine detected by a ground-based spectrometer were observed in coastal Antarctica (Saiz-Lopez et al., 2007) highlighting these coastal areas as an iodine hotspot. Enhanced sea ice bioproductivity during springtime and winter organic emissions have been suggested as the main sources of iodine in the Antarctic Peninsula (Atkinson et al., 2012; Granfors et al., 2014; Saiz-Lopez et al., 2015). Recent iodine instrumental measurements in the Antarctic coastal sea ice zone showed that I_2 dominates the iodine atom fluxes to the atmosphere (Atkinson et al., 2012). The same study revealed that iodocarbon concentrations above sea ice brines were over ten times greater than those of the sea water below.

The first measurements of bromine and iodine species (bromide Br^- and bromate BrO_3^- ; iodide I^- and iodate IO_3^-) in Antarctic ice were reported by Spolaor et al., (2012) indicating relatively stable concentrations of $100\text{-}200 \text{ pg Br}^- \text{ g}^{-1}$ and $5\text{-}32 \text{ pg I}^- \text{ g}^{-1}$ in Talos Dome ice from the early Holocene. Bromate and Iodate were not present above detection limits in these samples. Subsequently, total bromine concentrations in the Talos Dome ice core were reported for the past two glacial cycles, observing a depletion of bromine relative to the Br/Na ratio found in seawater during the last two glacial maxima (Spolaor et al., 2013b). The overall variability of bromine depletion corresponded well with a reconstruction of sea ice duration in the Victoria Land sector (Crosta et al., 2004), opening a basis for the further investigation of links between sea ice extent and bromine in polar ice cores. The seasonal nature of bromine enrichment in Antarctic ice was demonstrated by Spolaor et al. (2014), who reported spring/summer peaks of bromine enrichment and winter peaks of iodine concentration in Law Dome ice dating to 1910-1914 CE.

Reconstructions of Antarctic sea ice from ice core-based proxies have primarily been based on fluxes of sodium and/or methanesulphonic acid (MSA , CH_3SO_3^-) (e.g., Abram et al., 2013; Curran et al., 2003). In the EPICA Dome C ice core,



sodium concentrations were investigated by Rothlisberger et al. (2010) and compared to sea ice reconstructions from Southern Ocean marine sediment cores. For the last two glacial cycles, good correspondence was found between sea salt-derived sodium and the marine record. For reconstruction of sea ice area on decadal or even centennial scales, the influence of meteorological and depositional noise has been shown to be an important factor to consider especially for drill sites
5 located far inland such as Dome C (Levine et al., 2014).

In contrast, the presence of MSA in ice cores has been successfully linked to observed sea ice variability in a number of Antarctic ice cores (e.g., Abram et al., 2007; O'Dwyer et al., 2000). In some cases, the presence of MSA is either positively or negatively correlated with sea ice, depending on such factors as local wind direction, polynya and sea ice seasonality
10 (Abram et al., 2013). The longest reconstruction of sea ice extent using MSA has been reported for Law Dome, East Antarctica (Curran et al., 2003) covering the past 200 years and indicating a steady decrease in sea ice extent to the year 2000 C.E. Recent satellite observations report a slow increase in Antarctic sea ice over the past three decades (Parkinson and Cavalieri, 2012), and other MSA-based sea ice reconstructions support such observations (Thomas and Abram, 2016).

15 In this work, we report halogen deposition from the Dome Summit South (DSS), Law Dome ice core record covering the 20th century, with an emphasis on high-resolution measurements corresponding to the period since satellite observations of sea ice began. We examine correlations between sea ice area and bromine as well as halogen enrichment in the DSS Law Dome ice cores. The high rate of snow accumulation and regular year-round snowfall at Law Dome makes the site ideal for such a study, as well as the detailed MSA-based sea ice reconstruction already reported for the site. Although MSA
20 originates from a different emission source than bromine, both are related to sea ice area and hence should be expected to produce an overall similar pattern of sea ice variability on a multi-year or decadal scale.

2. Methods

25 2.1 Sample collection

2.1.1 Dome Summit South (DSS), Law Dome

The DSS ice cores are from Law Dome, East Antarctica. Law Dome is a small ice cap located approximately 120 km inland from the Wilkes Land coast (Fig. 1). The summit of Law Dome experiences relatively high and constant year-round
30 precipitation, providing clear seasonal variability in stable isotopes of water and ionic species (Curran et al., 1998). The summit of Law Dome features an accumulation rate of approximately 60 cm ice equivalent per year, with an average annual



temperature of -20° C. The precipitation is predominantly due to westerly cyclonic systems which produce a strong accumulation gradient from East (high accumulation) to west (low accumulation). The Law Dome summit is at an altitude of 1310 m asl, above approximately 1200 m of ice dating back to the last glacial (Morgan et al., 1997). The ice core samples were collected from the DSS site that is within a few hundred metres of the Law Dome summit, with the specific coordinates and sampling details described in the following sections. In all cases, the samples described here have been dated by identification and counting of annual cycles in stable isotopes of water (Morgan and van Ommen, 1997; Roberts et al., 2015) and ionic species (Curran et al., 1998) as well as synchronisation of well-dated volcanic eruption tie points (Plummer et al., 2012).

10 2.1.2 DSS0506

A 258 m deep ice core was drilled using a 20 cm diameter thermal drill near to the Law Dome summit ($66^{\circ}46'19.68''$ S, $112^{\circ}48'25.60''$ E) in November 2005 (Burn-Nunes et al., 2011). The core, designated DSS0506, was subsampled in October 2006 in a cold laboratory in a storage freezer in Hobart. For each ~ 1 metre long section of ice, a 35 mm x 35 mm stick was collected for chemical analysis, and subsequently decontaminated by chiselling with a microtome blade in an HEPA-filtered laminar flow bench in a freezer. All equipment used for the decontamination was repeatedly cleaned and stored in deionised water (Millipore MQ system, 18.2 MW/cm). The decontaminated samples were collected in polystyrene “Coulter counter” accuvettes and then melted for analysis by ion chromatograph. The remaining melted sample, usually 3 to 8 mL, was then refrozen and stored. In 2014 the remaining samples were sent to the University Ca’ Foscari of Venice for bromine determination. The depth range of DSS0506 samples reported here is from 19.7 m (1991 C.E.) to 72.5 m (1929 C.E.). The sampling resolution increased with depth, from 5 cm near the surface to 3 cm at depth, ensuring higher than monthly resolution at approximately 25 and 15 samples per year, respectively.

2.1.3 DSS1213

25

In austral summer 2012/2013, a 30 m firn core was drilled at DSS, Law Dome ($66^{\circ}46'21''$ S, $112^{\circ}48'40.59''$ E) using the 4-inch Kovacs Mark VI coring system (Roberts et al., 2015). The firn core was transported to Hobart, Australia, and subsampled in the freezer at the Australian Antarctic Division (AAD)/Antarctic Climate and Ecosystem CRC (ACE CRC). For each 1-metre length of firn, a 35 mm x 35 mm stick was cut and sent to the Trace Research Advanced Clean Environment (TRACE) laboratory at Curtin University of Technology, Perth, Western Australia, for bromine determination. A parallel 35 mm x 35 mm stick was decontaminated and analysed for stable isotopes of water and trace ions at the



AAD/ACE CRC in Hobart. Data covering the full depth range of the firn core are reported here, covering the period from summer 2012/2013 to late 1987 and overlapping with the DSS0506 record.

2.1.4 Law Dome traverse and DSS1516 snowpit

5

Another sampling expedition was conducted at Law Dome summit in February 2016, with snow surface samples collected during the traverse to the DSS site and from a 1-m snowpit. The DSS1516 snowpit (66°46'23.51" S, 112°48'40.59" E) was collected upwind from the traverse camp (designation: Waypoint A, 66°46'22.12" S, 112°48'28.19" E) and sampling was conducted immediately after the pit was prepared. Samples were collected every 3 cm by plunging pre-cleaned 50 mL polyethylene tubes into the pit wall. Stable isotopes of water ($\delta^{18}\text{O}$ and δD) measured in the parallel snow pit wall confirm that the 1 m sequence covers the period from winter (July) 2015 to February 2016.

In addition to the DSS1516 snowpit, surface snow samples were collected during a 1-day traverse from Casey station to the DSS Campsite A. Details of the sampling sites are included in Table S1 (supplementary material). Eleven samples were collected during the 114 km traverse, extending from an altitude of 500m asl to 1320 asl at the DSS1516 site. The samples were collected every 10 to 15 km by moving approximately 15 m upwind of the Hagglands traverse vehicle and plunging a polyethylene tube into the snow surface. The tubes were immediately sealed after sampling and were kept frozen until analysis. All samples collected during the traverse to and from the DSS1516 snowpit were sent to the TRACE laboratory at Curtin University of Technology for bromine analysis.

15
20

2.2 Halogen measurements

2.2.1 Australia

The DSS1213 1-metre sticks were cut and prepared in the TRACE laboratory located at Curtin University of Technology, Perth, Australia (Ellis et al., 2015). The 35 mm x 35 mm cross-section sticks were melted on a silicon carbide melter head at a melt rate of 5 cm/minute following the setup of McConnell et al (2002). The central melt line was directed to a Thermo Element XR ICP-SFMS fitted with cyclonic peltier-cooled spray chamber (2° C) and 400 uL/minute PFA ST nebulizer (both from ESI, Omaha, USA). The sample line was acidified with 2% ultrapure nitric acid and internal standard (4 ppb ^{115}In) immediately prior to its introduction to the plasma. All elements were determined at medium resolution (~4000 amu).

25
30



Law Dome traverse and DSS1516 snowpit samples were analysed discretely using a Seafast-II autosampler with syringe pump connected to the abovementioned analytical system. For these samples, iodine (^{127}I) was determined at low mass resolution (~ 300 amu) and the remaining elements at medium resolution (^{23}Na , ^{35}Cl , ^{79}Br). A 4 ppb ^{115}In internal standard was used at both mass resolutions. Analytical blanks and quality control standards were determined after every 10 samples analysed.

2.2.2 Italy

The DSS0506 and DSS1516 core samples were measured at the Environmental Analytical Chemistry laboratory of the University Ca'Foscari of Venice. The samples were stored in plastic vials and were kept frozen until analysis. For the DSS0506 samples, some of the polystyrene accuvettes were broken in transport and were found to be contaminated. Consequently, data corresponding to the years 1945-6, 1950-1, 1954-5 and 1963-4 are incomplete.

Similar to the Curtin University analysis, samples were measured on a Thermo Element2 ICP-SFMS instrument using a cyclonic peltier-cooled spray chamber (ESI, Omaha, USA). System cleaning and operational parameters have been described previously (Spolaor et al., 2013b). Elements were determined in low- (^{127}I) and medium-resolution (^{23}Na , ^{79}Br) with plasma stability evaluated by the continuous monitoring of ^{129}Xe . The sample line was thoroughly cleaned using 2% nitric acid (120 s) and UPW (120 s) between each analysis.

2.3 Ion chromatography measurements

Major and minor ions were determined at the AAD/ACE CRC laboratory in Hobart Australia following the established suppressed ion chromatographic methods (Curran and Palmer, 2001). Samples were stored and prepared in a HEPA-filtered cleanroom and all laboratory apparatus was cleaned using filtered deionized water (Millipore MQ system, 18.2 M Ω /cm). The MSA data covering the period 1920-1995 are those reported by Curran et al. (2003). Sodium data from the DSS main ice core record have been previously discussed by Palmer et al. (2001).

2.4 Sea ice area

Satellite based observations of sea ice extent and concentration have been used to evaluate the suitability of bromine and iodine as proxies for sea ice area reconstructions. We have calculated sea ice area as the product of sea ice concentration and



grid cell size for each grid cell in the two sectors considered. Note that this calculation produces a result that is slightly smaller than the sea ice extent, which is defined as the sum of grid cells containing at least 15% sea ice coverage. Sea ice area has been evaluated in in two ocean sectors adjacent to Law Dome is used for comparison: one to the west of Law Dome (90 to 110° E) and one to the east of Law Dome (110 to 130° E); as shown in Fig. 2. A strong East-to-West accumulation
5 gradient has been observed across Law Dome, hence it is expected that sea salts carried to Law Dome will predominantly originate from low pressure systems developing from the 90-110° E sector.

A discontinuous record of monthly sea ice area has been calculated from a series of satellite-based sensors, covering the period from 1973 to 2015 with missing years for 1977 and 1978. Sea ice area for the period 1973 to 1977 was determined
10 from daily brightness temperatures monitored by the ESMR instrument mounted on the NIMBUS-5 satellite (Parkinson et al., 2004). For the period January 1979 to May 2015, sea ice observations were obtained from the SMMR and SSM/I and SSMIS instruments mounted on various satellite platforms (Cavalieri et al., 1996, updated yearly). These data are freely available from the US National Snow and Ice Data Centre (NSIDC) website (Cavalieri et al., 1999; Fetterer et al., 2002, updated daily).

15 First year sea ice (FYSI) area has been calculated as the difference between the late-summer (February/March) minimum and late-winter (September/October) maximum of sea ice area occurring each year. FYSI data series' calculated for the 90-110° E and 110-130° E sectors are shown in Fig. 3. Also shown in Fig. 3 are two other publicly available datasets reporting sea ice extent (not sea ice area), largely calculated from the same satellite observations. The first dataset, here referred to as 'Jacka
20 SIE', reports monthly observations of the northernmost sea ice edge (SIE) for 10° sectors of longitude around Antarctica over the period 1973-1998. The data are available online (www.antrc.utas.edu.au/jacka/climate.html) and were employed by Curran et al. (2003) to validate their MSA-based Law Dome sea ice reconstruction. The second dataset is produced by National Snow and Ice Data Centre (NSIDC) and offers near-daily sea ice extent over the period 1978-2013 for Antarctica. The data are divided into 5 Antarctic sectors, of which the "Pacific Ocean" sector encompasses 90-160° E and includes Law
25 Dome. The Jacka SIE and NSIDC datasets are shown to demonstrate their good correspondence with the FYSI data reported here for regression analysis with Law Dome bromine data. In Fig. 3, we also plot the sum of the 90-110° E and 110-130° E FYSI datasets to allow better comparison to those of Jacka SIE and NSIDC.

3. Results and discussion

30



3.1 Halogen and sodium records

Mean bromine, iodine and sodium glaciochemical concentrations (1927-2012 CE for Br and Na, 1927-1989 CE for I) at DSS were comparable to previously reported values for Law Dome (Curran et al., 1998; Spolaor et al., 2014). Considering annual averages over the period 1927-2012, we find average concentrations of 88 ± 45 (1σ) ng g^{-1} for Na and 2.9 ± 2.7 (1σ) ng g^{-1} for Br. For iodine, the average for the period 1927-1989 is 0.061 ± 0.023 ng g^{-1} (1σ , $n=62$). As may be expected from the “spiky” nature of the data, the geometric means of the data (81 ng Na g^{-1} , 2.3 ng Br g^{-1} , 0.057 ng I g^{-1}) are 5 to 20% lower than the arithmetic means. Annually-averaged non-sea salt Br (nssBr) concentrations average 2.4 ng g^{-1} (geomean 1.6 ng g^{-1}) comparable to values reported previously for Law Dome (Spolaor et al., 2014). Sodium concentrations are also in good agreement with previously reported values of 3.47 ± 3.03 (1σ) meq L^{-1} (80 ± 70 ng g^{-1}) (Curran et al., 1998).

The bromine, iodine and sodium time series records determined for DSS firn and ice cores are shown in Fig. 4. No significant trend is present in any of the timeseries. The sodium data are representative of sea salt inputs from the Southern Ocean to the site whereas bromine is known to be subject to enhancement in photochemical ‘bromine explosion’ events. We quantify the strength of such photochemical enrichment by calculating the bromine enrichment (Br_{enr}) beyond the bromine/sodium abundance ratio found ubiquitously in seawater [$\text{Br}/\text{Na}=0.006$; Turekian (1968)]. Following the well-established methodology of Spolaor and colleagues (Spolaor et al., 2013a; Spolaor et al., 2014; Spolaor et al., 2016) we calculate $\text{Br}_{\text{enr}} = \text{Br}_{\text{conc}}/(\text{Na}_{\text{conc}} * 0.006)$, where Br_{conc} and Na_{conc} respectively describe the concentrations of Br and Na measured in a sample. For iodine enrichment (I_{enr}) we apply the same enrichment calculation but using the iodine/sodium ratio in seawater of 5.93×10^{-6} (Turekian, 1968). Iodine and bromine enrichment data and their relation to sea ice variability will be discussed in the following sections.

There appears to be less interannual variability in the DSS1213 Br record, with respect to the DSS0506 record. This is likely due to aliasing by the ice core melter system, which had a flow path ~ 5 times that of the discrete sampling system. The average values of Br_{enr} and Br_{conc} are similar for the two cores but the variance of annual averages is much greater for the DSS0506 samples (Table 1). For sodium, there is no substantial difference in average concentration but the opposite trend is found for variance, with greater variance in the DSS1213 data. We attribute this difference in variance to the different sampling and analytical techniques applied to each core – DSS0506 was sampled by discrete chiselling and DSS1213 sampled by continuous melting. Sodium does not have a significant memory effect and the higher variance found by the ice core melter is expected due to the higher depth-resolution of the melter system compared to discrete sampling. Despite the apparent aliasing of the DSS1213 Br record, the two records show good agreement in the overlap period from calendar 1988 to 1989 (Fig. 4). A double peak in Br was found with the initial peak in the DSS0506 core leading the DSS1213 record by approximately 2 weeks (from comparison of the time scales), which is well within the sub-annual dating error.



3.2 Bromine and first year sea ice

Considering the known relationships between emissions of bromine and seasonal sea ice area, we investigated the reliability of bromine, and bromine enrichment, as a proxy for regional seasonal sea ice area adjacent to Law Dome. To reduce and linearize the variability in the Br_{enr} data, which may act to artificially increase the correlation, we use the natural logarithm of Br_{enr} for correlation to FYSI data. An additional reason for applying a logarithmic transformation is due to the exponential nature of the “bromine explosion” process occurring above the bromine-rich FYSI surface: in each stage of the explosion, one reactive bromine species (HOBr) is consumed in the process of liberating Br_2 from the sea ice surface. As Br_2 is the reactive precursor to two subsequent bromine explosion multiphase reactions, the process develops exponentially. Correlation tests have been performed using different subsets of the $\ln(Br_{enr})$ data; such as summer-summer (calendar year), winter-winter (July-June) and spring-only (August-October) intervals. The FYSI data used for correlation has been described in Sect. 2.4. Note that the optimal correlation is found when $\ln(Br_{enr})$ is compared to the FYSI value from the previous year. This is due to the timing of formation of sea ice in the Antarctic (from March to September) occurring, by necessity, earlier than the springtime bromine explosion that occurs in the following calendar year.

A summary of the correlation analysis between Law Dome bromine enrichment and FYSI is shown in Table 2. We observe firstly that $\ln(Br_{enr})$ is consistently better correlated with the 90-110°E sector than for the 110-130°E sector. Such a finding is consistent with the westerly circulation around Antarctica, despite the individual cyclonic systems producing an east-to-west deposition gradient across Law Dome. It is also consistent that the 80-140° E sector demonstrated the strongest correlation between sea ice extent and MSA concentrations at Law Dome (Curran et al., 2003). The strongest correlation (r^2 0.322, $p < 0.001$) found here is between $\ln(Br_{enr})$ and 90-110° E sector FYSI for the summer-summer calendar year period, although a reasonable correlation is also observed between 90-110° E FYSI and the winter-winter interval (r^2 0.24, $p < 0.01$). Such a finding is counter-intuitive because the bromine explosion occurs primarily in spring/summer and should be most completely captured in the winter-winter interval. As has been demonstrated thoroughly by Levine et al. (2014), meteorological transport variability, postdepositional remobilization and other “noise effects” can have a strong influence on the reliability of sea salt deposition. Hence it may be that the summer-summer interval produces a marginally stronger correlation with 90-110° E FYSI due to the smoothing effect caused by the averaging of consecutive spring/summer periods. It is important to recognise that irrespective of the seasonality, Br enrichment data show a consistent and significant correlation to FYSI in the vicinity of Law Dome.



3.3 Bromine enrichment as a sea ice proxy

On the basis of the significant correlation between bromine enrichment at Law Dome and 90-110° E FYSI, we consider the implications for reconstructing past sea ice area at Law Dome. Figure 5 shows Law Dome $\ln(\text{Br}_{\text{enr}})$ and MSA (Curran et al., 2003) since 1927 C.E. as well as the 90-110° E FYSI data plotted as an anomaly from the average of the data, to better display FYSI trends. We firstly note that a selection of running-mean smoothing filters have been applied to such data previously, such as 3- and 20- year means (Curran et al., 2003) and 11-year means (Abram et al., 2010). Here we follow the latter and show 11-year means as well as the individual annual data points.

When comparing two proxies purporting to represent the same phenomenon it is vital to consider the different physical processes involved in the proxy generation, transport and deposition. We note that MSA is produced biologically and, for the Law Dome sector, has been quantitatively linked to the opening of sea ice-covered seawater during the summer and autumn seasons. Bromine enrichment occurs primarily in spring/summer and is dependent upon the presence of FYSI (Saiz-Lopez and von Glasow, 2012). Hence, the differences in seasonal patterns, factors influencing biological growth, relations to sea ice and transport efficacy will be also considered when comparing bromine enrichment and MSA trends at Law Dome.

Some differences are seen among the sea ice trends indicated by MSA and bromine at Law Dome over the 20th century (Fig. 5). Both proxies display substantial multidecadal variability, so any long-term trend is here treated with caution. In the cases of both bromine and MSA, simple linear regression indicates small declining trends for both species. Bromine enrichment values are greater during the period 1940-1950 and 1975-1985 while the highest MSA concentrations are observed during the periods 1920-1930 and 1945-1955. Bromine and MSA both point toward greater sea ice area during the period from 1945 to 1950 and agree on a general decrease in area over the 20th century. Bromine and MSA show a positive inflection during the period 1975-1985, although the change is stronger in bromine, where enrichment values return to levels similar to 1945. The magnitude of change in MSA is much smaller. FYSI displayed positive anomalies prior to 1985 and have displayed negative anomalies in the last decades. The agreement between the bromine enrichment and the FYSI anomalies during the last 30 years (Fig. 5) supports our interpretation of Br_{enr} as a proxy for sea ice area.

3.4 Iodine enrichment

Iodine enrichment in sea ice could be explained by complex heterogeneous reactions that take place above seasonal sea ice releasing gas phase iodine and particulate species. Even though peak I concentrations are found in winter at Law Dome (Spolaor et al., 2014), the peak I_{enr} signal occurs in summer, synchronously to that of B_{enr} . There is no significant correlation



between Br_{enr} and I_{enr} signals on an annual basis ($r^2=0.05$, $p<0.1$). This lack of significant correlation might be related to the different iodine emissions and recycling mechanisms over sea ice: i) release of iodine from sea-ice enhanced bioproductivity and subsequent upwards migration through brine channels (Saiz-Lopez et al., 2015); ii) photochemical reactions over iodate frozen salts (Spolaor et al., 2012) and ii) atmospheric release of gas phase iodine from triiodide production via iodide oxidation in frozen solution (Kim et al., 2016). Another indicator of the complex ocean-sea ice-atmosphere interrelation arises from the statistical comparison with FYSI records (Table 2). The significance levels for I_{enr} are consistently poorer than for Br_{enr} , and there is less consistency in the FYSI source region. The most significant correlation of I_{enr} is between the summer-summer (calendar year) averaged signal and the 110-130° E FYSI sector.

10 Correlation between I_{enr} and Br_{enr} for the 11-year smoothed data is significant ($r^2=0.269$, $p<0.001$) suggesting a long-term (decadal scale) common driver controlling halogens deposition in coastal Antarctica. The iodine enrichment time series shows a similar pattern to that of bromine enrichment, with higher values particularly during the 1940s and 1970s (Fig. 6). These periods coincide with rapid changes in the Interdecadal Pacific Oscillation (IPO) phase from positive to negative in the 1940s and back from negative to positive in the 1970s. Impurities deposited at Law Dome have been demonstrated to

15 faithfully reflect IPO variability (Vance et al., 2015) and reanalysis data indicates a strong IPO signal in the Indian Ocean (Vance et al., 2016). Thus the overall correlation between iodine and bromine enrichment may be linked to decadal-scale states of the atmosphere-ocean-sea ice system in the Indian sector of the Southern Ocean.

3.5 Bromine seasonality

20

Due to the availability of consistent and highly resolved data from the DSS1213 core, it is possible to investigate seasonal distributions of sodium and bromine at Law Dome. The seasonal cycle of major and minor ions has been previously reported for Law Dome (Curran et al., 1998) but for bromine only four years are available (Spolaor et al., 2014). Here we present the DSS1213 record, which covers the period 1987 to 2012. The seasonality of sodium and Br_{enr} are shown in Fig. 7. Sodium

25 shows a broad period of high concentrations from April to September, with lower concentrations during the summer. This pattern broadly agrees with that reported by Curran et al., (1998) although those authors found a sharper sodium peak in late winter, associated with both the local sea ice maximum and the strongest local wind fields. We note also that the highest concentration of sodium is found in March-April and is likely due to one of ‘a small number of large storm events which occasionally occur early in the year, lofting higher concentrations of sea-salt aerosol onto the summit of the dome’ (Curran

30 et al., 1998).

The trend observed for Br_{enr} is one of lower concentrations in winter and higher concentrations from November to February. There is high variability in the sodium signal throughout the year, whereas the Br_{enr} signal is most variable during the



summer months. The seasonality of Br_{enr} found here confirms that suggested by the four-year data series presented by Spolaor et al. (2014), with a broad summer peak in Br_{enr} . Satellite observations of atmospheric BrO in polar regions suggest an early spring peak in bromine activity in Antarctica (Spolaor et al., 2014), thereby implying that additional processes may be occurring in the snowpack during the summer after the peak atmospheric bromine explosion has occurred. While
5 snowpack remobilisation at Law Dome is minimal, it might be the case that photochemically-driven heterogenous recycling of bromine occurs in the snowpack after the springtime occurrence of the bromine explosion. This effect requires further investigation, from satellite and ground-based observations to weekly surface snow sampling, in order to be fully characterised and understood.

10 3.6 Bromine deposition across Law Dome

Variability in sodium and bromine was investigated along the transect line from Casey station to the Law Dome summit. The traverse route is indicated in Fig. 1, where 11 samples were collected over a period of 4 hours on the 10th February 2016. Conditions were clear with low wind and good visibility. Details of the sampling sites are included in Table S1
15 (supplementary material). The sodium and bromine results for each station are shown in Fig. 8.

Substantial variability can be seen along the traverse, with somewhat greater sodium concentrations closer to the coast and a tendency toward greater bromine enrichment values farther away from the coast. It should be noted that the sampling was undertaken on the ‘lee side’ of Law Dome, across a region which generally exhibits low annual accumulation on the order of
20 $<200 \text{ kg m}^{-2}$. The final 25 km of the traverse sees a threefold-increase in annual accumulation to $>600 \text{ kg m}^{-2}$. The data presented here represent a first attempt to capture the surface variability of sodium and bromine across Law Dome. Future expeditions to Law Dome should incorporate a procedure for surface sampling along the traverse line and ideally further east toward the origin of the precipitation pathway over Law Dome.

25 4. Conclusions

The Law Dome site is ideal for studies of sea ice proxies, due to the regular and high level of annual precipitation allowing detailed studies of seasonality as well as the optimal preservation conditions. We find here that bromine enrichment over the past century displays a comparable trend to that of MSA, which has been previously used for reconstruction of local sea ice
30 extent. The bromine-based reconstruction of the sea ice area in the 90110° E Antarctic sector indicates a significant sea ice



area reduction within the 20th century. In agreement with satellite observations sea ice area slightly increased again since 1990 but stays still well below the values at the beginning of the time series.

In agreement with a previous study of halogen seasonality at Law Dome, we find that both bromine and iodine enrichment display regular seasonality with a broad summer peak. Iodine enrichment is significantly correlated to bromine enrichment on decadal scales but not annual scales, suggesting a greater level of meteorological disturbance to the iodine signal despite a common long-term enrichment source, which we propose to be first-year sea ice.

More extensive sampling across Law Dome and further inland should be considered in future field seasons. Samples collected during a traverse from Casey station to Law Dome DSS site display a consistent increase in deposition fluxes from west to east, as expected from the easterly cyclonic systems responsible for the precipitation at Law Dome. Additional traverse data should be collected at the next available opportunity and ideally, the traverse should be extended over the dome summit and onto the eastern side of the dome. The Law Dome halogens record presented here should be extended further back in time and similar studies should be undertaken at other Antarctic locations, to ensure consistency and validation of the sea ice reconstruction presented here.

Data availability

Data will be made publicly available online through the NOAA Paleoclimatology database and PANGAEA data repository.

Acknowledgements

The research leading to these results has received funding from the European Research Council under the European Union's Seventh Framework Programme (FP7/2007-2013) grant agreement #610055 “Ice2ice”. The Australian Antarctic Division provided funding and logistical support for the DSS ice cores (AAS projects 4061 and 4062). G. Spreen has been supported by the Institutional Strategy of the University of Bremen, funded by the German Excellence Initiative. All correlations and associated confidence levels reported here have been calculated using the program R via the RStudio interface.

References



- Abram, N. J., Mulvaney, R., Wolff, E. W., and Mudelsee, M.: Ice core records as sea ice proxies: An evaluation from the Weddell Sea region of Antarctica, *J. Geophys. Res.*, 112, doi: 10.1029/2006JD008139, 2007.
- Abram, N. J., Wolff, E. W., and Curran, M. A. J.: A review of sea ice proxy information from polar ice cores, *Quaternary Sci. Rev.*, 79, 168-183, doi: 10.1016/j.quascirev.2013.01.011, 2013.
- 5 Atkinson, H. M., Huang, R. J., Chance, R., Roscoe, H. K., Hughes, C., Davison, B., Schönhardt, A., Mahajan, A. S., Saiz-Lopez, A., Hoffmann, T., and Liss, P. S.: Iodine emissions from the sea ice of the Weddell Sea, *Atmos. Chem. Phys.*, 12, 11229-11244, doi: 10.5194/acp-12-11229-2012, 2012.
- Brooks, S. B., Saiz-Lopez, A., Skov, H., Lindberg, S. E., Plane, J. M. C., and Goodsite, M. E.: The mass balance of mercury in the springtime arctic environment, *Geophys. Res. Lett.*, 33, doi: 10.1029/2005GL025525, 2006.
- 10 Burn-Nunes, L. J., Vallelonga, P., Loss, R. D., Burton, G., Moy, A., Curran, M., Hong, S., Smith, A. M., Edwards, R., Morgan, V., and Rosman, K. J. R.: Seasonal variability in the input of lead, barium and indium to Law Dome, Antarctica, *Geochim. Cosmochim. Acta*, 75, 1-20, doi: 10.1016/j.gca.2010.09.037, 2011.
- Cavalieri, D. J., Parkinson, C. L., Gloersen, P., and Zwally, H. J.: Sea Ice Concentrations from Nimbus-7 SMMR and DMSP SSM/I-SSMIS Passive Microwave Data, Version 1, NASA National Snow and Ice Data Center Distributed Active Archive Center, Boulder, Colorado USA, doi: 10.5067/8GQ8LZQVL0VL, 1996, updated yearly.
- 15 Cavalieri, D. J., Parkinson, C. L., Gloersen, P., Comiso, J. C., and Zwally, H. J.: Deriving long-term time series of sea ice cover from satellite passive-microwave multisensor data sets, *J. Geophys. Res.*, 104, 15803-15814, doi: 10.1029/1999JC900081, 1999.
- 20 Crosta, X., Sturm, A., Armand, L., and Pichon, J.-J.: Late Quaternary sea ice history in the Indian sector of the Southern Ocean as recorded by diatom assemblages, *Mar. Micropaleontol.*, 50, 209-223, doi: 10.1016/S0377-8398(03)00072-0, 2004.
- Curran, M., and Palmer, A. S.: Suppressed ion chromatography methods for the routine determination of ultra low level anions and cations in ice cores, *J. Chromatogr. A*, 919, 1-7, doi: 10.1016/S0021-9673(01)00790-7, 2001.
- Curran, M. A. J., van Ommen, T. D., and Morgan, V. I.: Seasonal characteristics of the major ions in the high-accumulation 25 Dome Summit South ice core, Law Dome, Antarctica, *Ann. Glaciol.*, 27, 385-390, doi: 10.3198/1998AoG27-1-385-390, 1998.
- Curran, M. A. J., Tas D. van Ommen, Morgan, V. I., Phillips, K. L., and Palmer, A. S.: Ice core evidence for Antarctic sea ice decline since the 1950s, *Science*, 302, 1203-1206, doi: 10.1126/science.1087888, 2003.
- 30 Ellis, A., Edwards, R., Saunders, M., Chakrabarty, R. K., Subramanian, R., van Riessen, A., Smith, A. M., Lambrinidis, D., Nunes, L. J., Vallelonga, P., Goodwin, I. D., Moy, A. D., Curran, M. A. J., and van Ommen, T. D.: Characterizing black carbon in rain and ice cores using coupled tangential flow filtration and transmission electron microscopy, *Atmos. Meas. Tech.*, 8, 3959-3969, doi: 10.5194/amt-8-3959-2015, 2015.
- Fetterer, F., Knowles, K., Meier, W., and Savoie, M.: Sea Ice Index, Version 1. [1978-2013]. Boulder, Colorado USA. NSIDC: National Snow and Ice Data Center. [March 2016], doi: 10.7265/N5QJ7F7W, 2002, updated daily.
- 35 Granfors, A., Ahnoff, M., Mills, M. M., and Abrahamsson, K.: Organic iodine in Antarctic sea ice: A comparison between winter in the Weddell Sea and summer in the Amundsen Sea, *J. Geophys. Res.*, 119, 2276-2291, doi: 10.1002/2014JG002727, 2014.
- Hylander, L. D., and Goodsite, M. E.: Environmental costs of mercury pollution, *Sci. Total Env.*, 368, 352-370, doi: 10.1016/j.scitotenv.2005.11.029, 2006.
- 40 Impey, G. A., Shepson, P. B., Hastie, D. R., Barrie, L. A., and Anlauf, K. G.: Measurements of photolyzable chlorine and bromine during the Polar Sunrise Experiment 1995, *J. Geophys. Res.*, 102, 16005-16010, doi: 10.1029/97JD00851, 1997.
- Kim, K., Yabushita, A., Okumura, M., Saiz-Lopez, A., Cuevas, C. A., Blaszcak-Boxe, C. S., Min, D. W., Yoon, H.-I., and Choi, W.: Production of Molecular Iodine and Tri-iodide in the Frozen Solution of Iodide: Implication for Polar Atmosphere, *Environ. Sci. Technol.*, 50, 1280-1287, doi: 10.1021/acs.est.5b05148, 2016.
- 45 Levine, J. G., Yang, X., Jones, A. E., and Wolff, E. W.: Sea salt as an ice core proxy for past sea ice extent: A process-based model study, *J. Geophys. Res.-Atmos.*, 119, 5737-5756, doi: 10.1002/2013JD020925, 2014.
- McConnell, J. R., Lamorey, G. W., Lambert, S. W., and Taylor, K. C.: Continuous ice-core chemical analyses using inductively coupled plasma mass spectrometry, *Environ. Sci. Technol.*, 36, 7-11, doi: 10.1021/es011088z, 2002.
- 50 Morgan, V., and van Ommen, T. D.: Seasonality in late-Holocene climate from ice-core records, *The Holocene*, 7, 351-354, doi: 10.1177/095968369700700312, 1997.



- Morgan, V., Wookey, C. W., Li, J., van Ommen, T. D., Skinner, W., and Fitzpatrick, M. F.: Site information and initial results from deep ice drilling on Law Dome, Antarctica, *J. Glaciol.*, 43, 3-10, doi: 10.3198/1997JoG43-143-3-10, 1997.
- Nerentorp Mastromonaco, M., Gärdfeldt, K., Jourdain, B., Abrahamsson, K., Granfors, A., Ahnoff, M., Dommergue, A., Méjean, G., and Jacobi, H. W.: Antarctic winter mercury and ozone depletion events over sea ice, *Atmos. Environ.*, 129, 125-132, doi: 10.1016/j.atmosenv.2016.01.023, 2016.
- 5 O'Dwyer, J., Isaksson, E., Vinje, T., Jauhiainen, T., Moore, J., Pohjola, V., Vaikmäe, R., and van de Wal, R. S. W.: Methanesulfonic acid in a Svalbard Ice Core as an indicator of ocean climate, *Geophys. Res. Lett.*, 27, 1159-1162, doi: 10.1029/1999gl011106, 2000.
- Palmer, A. S., van Ommen, T. D., Curran, M. A. J., Morgan, V. I., Souney, J. M., and Mayewski, P. A.: High precision dating of volcanic events (A.D. 1301-1995) using ice cores from Law Dome, Antarctica, *J. Geophys. Res.*, 106, 28089-28095, doi: 10.1029/2001JD000330, 2001.
- 10 Parkinson, C. L., Comiso, J. C., and Zwally, H. J.: Nimbus-5 ESMR Polar Gridded Sea Ice Concentrations, Version 1, in, edited by: Meier, W., and Stroeve, J., NASA National Snow and Ice Data Center Distributed Active Archive Center, Boulder, Colorado USA, 2004.
- 15 Parkinson, C. L., and Cavalieri, D. J.: Antarctic sea ice variability and trends, 1979--2010, *The Cryosphere*, 6, 871-880, doi: 10.5194/tc-6-871-2012, 2012.
- Plummer, C. T., Curran, M. A. J., van Ommen, T. D., Rasmussen, S. O., Moy, A. D., Vance, T. R., Clausen, H. B., Vinther, B. M., and Mayewski, P. A.: An independently dated 2000-yr volcanic record from Law Dome, East Antarctica, including a new perspective on the dating of the 1450s CE eruption of Kuwae, Vanuatu, *Clim. Past*, 8, 1929-1940, doi: 10.5194/cp-8-1929-2012, 2012.
- 20 Pratt, K. A., Custard, K. D., Shepson, P. B., Douglas, T. A., Pohler, D., General, S., Zielcke, J., Simpson, W. R., Platt, U., Tanner, D. J., Gregory Huey, L., Carlsen, M., and Stirm, B. H.: Photochemical production of molecular bromine in Arctic surface snowpacks, *Nature Geosci.*, 6, 351-356, doi: 10.1038/ngeo1779, 2013.
- 25 Roberts, J., Plummer, C., Vance, T., van Ommen, T., Moy, A., Poynter, S., Treverrow, A., Curran, M., and George, S.: A 2000-year annual record of snow accumulation rates for Law Dome, East Antarctica, *Clim. Past*, 11, 697-707, doi: 10.5194/cp-11-697-2015, 2015.
- Röthlisberger, R., Crosta, X., Abram, N. J., Armand, L., and Wolff, E. W.: Potential and limitations of marine and ice core sea ice proxies: an example from the Indian Ocean sector, *Quaternary Sci. Rev.*, 29, 296-302, doi: 10.1016/j.quascirev.2009.10.005, 2010.
- 30 Saiz-Lopez, A., Mahajan, A. S., Salmon, R. A., Bauguitte, S. J. B., Jones, A. E., Roscoe, H. K., and Plane, J. M. C.: Boundary Layer Halogens in Coastal Antarctica, *Science*, 317, 348-351, doi: 10.1126/science.1141408, 2007.
- Saiz-Lopez, A., Plane, J. M. C., Baker, A. R., Carpenter, L. J., von Glasow, R., Gomez Martin, J. C., McFiggans, G., and Saunders, R. W.: Atmospheric Chemistry of Iodine, *Chem. Rev.*, 112, 1773-1804, doi: 10.1021/cr5006638, 2012.
- 35 Saiz-Lopez, A., and von Glasow, R.: Reactive halogen chemistry in the troposphere, *Chem. Soc. Rev.*, 41, 6448-6472, doi: 10.1039/C2CS35208G, 2012.
- Saiz-Lopez, A., Baidar, S., Cuevas, C. A., Koenig, T. K., Fernandez, R. P., Dix, B., Kinnison, D. E., Lamarque, J., Campos, T. L., and Volkamer, R.: Injection of iodine to the stratosphere, *Geophys. Res. Lett.*, 42, 1-8, doi: 10.1002/2015GL064796, 2015.
- Simpson, W. R., von Glasow, R., Riedel, K., Anderson, P., Ariya, P., Bottenheim, J., Burrows, J., Carpenter, L. J., Frieß, U., Goodsite, M. E., Heard, D., Hutterli, M., Jacobi, H. W., Kaleschke, L., Neff, B., Plane, J., Platt, U., Richter, A., Roscoe, H., Sander, R., Shepson, P., Sodeau, J., Steffen, A., Wagner, T., and Wolff, E.: Halogens and their role in polar boundary-layer ozone depletion, *Atmos. Chem. Phys.*, 7, 4375-4418, doi: 10.5194/acp-7-4375-2007, 2007.
- 40 Simpson, W. R., Brown, S. S., Saiz-Lopez, A., Thornton, J. A., and Glasow, R. v.: Tropospheric Halogen Chemistry: Sources, Cycling, and Impacts, *Chem. Rev.*, 115, 4035-4062, doi: 10.1021/cr5006638, 2015.
- 45 Spolaor, A., Vallenga, P., Gabrieli, J., Kehrwald, N., Turetta, C., Cozzi, G., Plane, J. M. C., Boutron, C., and Barbante, C.: Speciation analysis of iodine and bromine at picogram-per-gram levels in Polar Ice, *Anal. Bioanal. Chem.*, 405, 647-654, doi: 10.1007/s00216-012-5806-0, 2012.
- 50 Spolaor, A., Gabrieli, J., Martma, T., Kohler, J., Björkmann, M., Isaksson, E., Varin, C., Vallenga, P., Plane, J. M. C., and Barbante, C.: Sea ice dynamics influence halogen deposition to Svalbard, *The Cryosphere*, 7, 1645-1658, doi: 10.5194/tc-7-1645-2013, 2013a.



- Spolaor, A., Vallelonga, P., Plane, J. M. C., Kehrwald, N., Gabrieli, J., Varin, C., Turetta, C., Cozzi, G., Kumar, R., Boutron, C., and Barbante, C.: Halogen species record Antarctic sea ice extent over glacial-interglacial periods, *Atmos. Chem. Phys.*, 13, 6623-6635, doi: 10.5194/acp-13-6623-2013, 2013b.
- 5 Spolaor, A., Vallelonga, P., Gabrieli, J., Martma, T., Björkman, M. P., Isaksson, E., Cozzi, G., Turetta, C., Kjær, H. A., Curran, M. A. J., Moy, A. D., Schönhardt, A., Blechschmidt, A. M., Burrows, J. P., Plane, J. M. C., and Barbante, C.: Seasonality of halogen deposition in polar snow and ice, *Atmos. Chem. Phys.*, 14, 9613-9622, doi: 10.5194/acp-14-9613-2014, 2014.
- Spolaor, A., Opel, T., McConnell, J. R., Maselli, O. J., Spreen, G., Varin, C., Kirchgeorg, T., Fritzsche, D., Saiz-Lopez, A., and Vallelonga, P.: Halogen-based reconstruction of Russian Arctic sea ice area from the Akademii Nauk ice core (Severnaya Zemlya), *The Cryosphere*, 10, 245-256, doi: 10.5194/tc-10-245-2016, 2016.
- 10 Thomas, E. R., and Abram, N. J.: Ice core reconstruction of sea ice change in the Amundsen-Ross Seas since 1702 A.D., *Geophys. Res. Lett.*, 43, 5309-5317, doi: 10.1002/2016GL068130, 2016.
- Turekian, K. K.: *Oceans*, Prentice-Hall, New Jersey, 120 pp., 1968.
- 15 Vance, T. R., Roberts, J. L., Plummer, C. T., Kiem, A. S., and van Ommen, T. D.: Interdecadal Pacific variability and eastern Australian mega-droughts over the last millennium, *Geophys. Res. Lett.*, 42, 129-137, doi: 10.1002/2014GL062447, 2015.
- Vance, T. R., Roberts, J. L., Moy, A. D., Curran, M. A. J., Tozer, C. R., Gallant, A. J. E., Abram, N. J., van Ommen, T. D., Young, D. A., Grima, C., Blankenship, D. D., and Siegert, M. J.: Optimal site selection for a high-resolution ice core record in East Antarctica, *Clim. Past*, 12, 595-610, doi: 10.5194/cp-12-595-2016, 2016.
- 20 Zhao, X., Strong, K., Adams, C., Schofield, R., Yang, X., Richter, A., Friess, U., Blechschmidt, A.-M., and Koo, J.-H.: A case study of a transported bromine explosion event in the Canadian high arctic, *J. Geophys. Res. Atmos.*, 121, 457-477, doi: 10.1002/2015JD023711, 2016.



Table 1. Statistical summary of time series data presented from Law Dome Dome Summit South (DSS) ice cores.

Core designation	Time interval	# years	Sodium (ppb)		Bromine (ppb)		Ln(Brconc)		Ln (Brenr)	
			Mean	variance	Mean	variance	Mean	variance	Mean	variance
DSS1213	1987-2012	25	115	4355	2	0.2	0.67	0.06	1.8	0.1
DSS0506	1927-1986	59	77	571	3.3	9.7	0.88	0.57	2.5	0.6

5



Table 2. Correlations between bromine and iodine enrichments and First year Sea Ice (FYSI) areas calculated for two sectors adjacent to Law Dome. Correlations that are significant at the 99% level or above are shown in bold.

Ln(Br _{enr})	# years	FYSI 90-110 °E		FYSI 110-130 °E	
		r ²	p-value	r ²	p-value
Jan-Dec (summer-summer)	36	0.322	<0.001	0.001	ns
Jul-Jun (winter-winter)	36	0.24	<0.01	0.15	<0.05
Sep-Nov (Spring only)	36	0.10	<0.1	0.004	ns

I _{enr}	# years	FYSI 90-110 °E		FYSI 110-130 °E	
		r ²	p-value	r ²	p-value
Jan-Dec (summer-summer)	15	0.16	<1	0.42	<0.01
Jul-Jun (winter-winter)	15	0.23	<0.1	0.12	ns
Sep-Nov (Spring only)	15	0.03	ns	0.01	ns

5

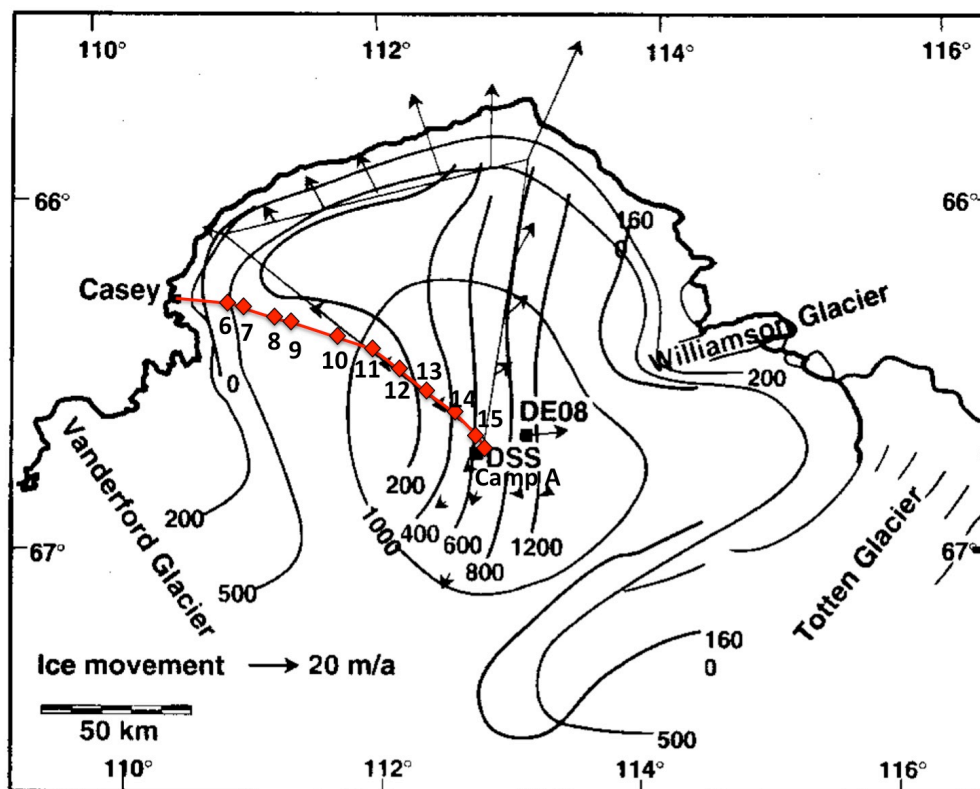
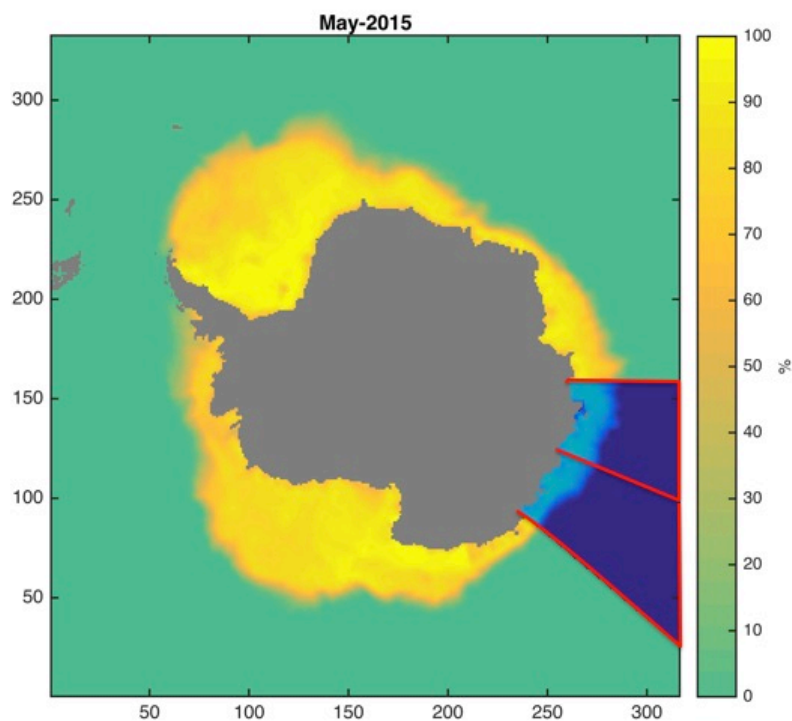
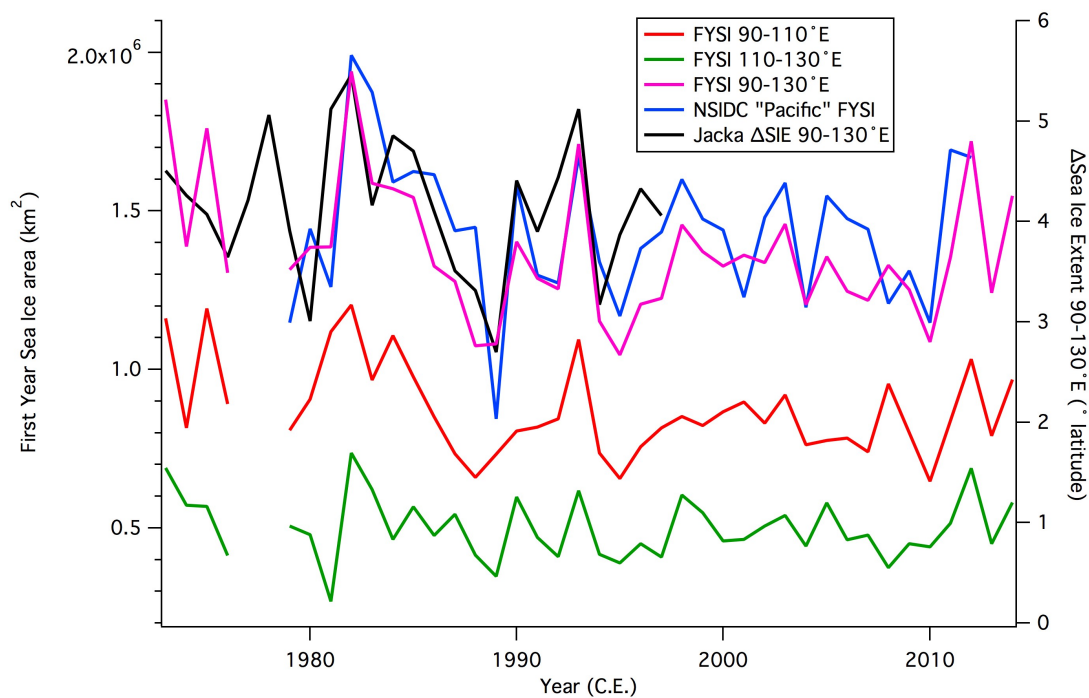


Figure 1: Map of Law Dome with contours of elevation (m asl) and accumulation ($\text{kg m}^{-2} \text{a}^{-1}$). The red line indicates the traverse route from Casey station to Camp A located near the Law Dome Summit. Red diamonds indicate the LDT surface snow sampling stations. DSS1516, DSS1213 and DSS0506 sampling sites are all in the vicinity of Camp A.



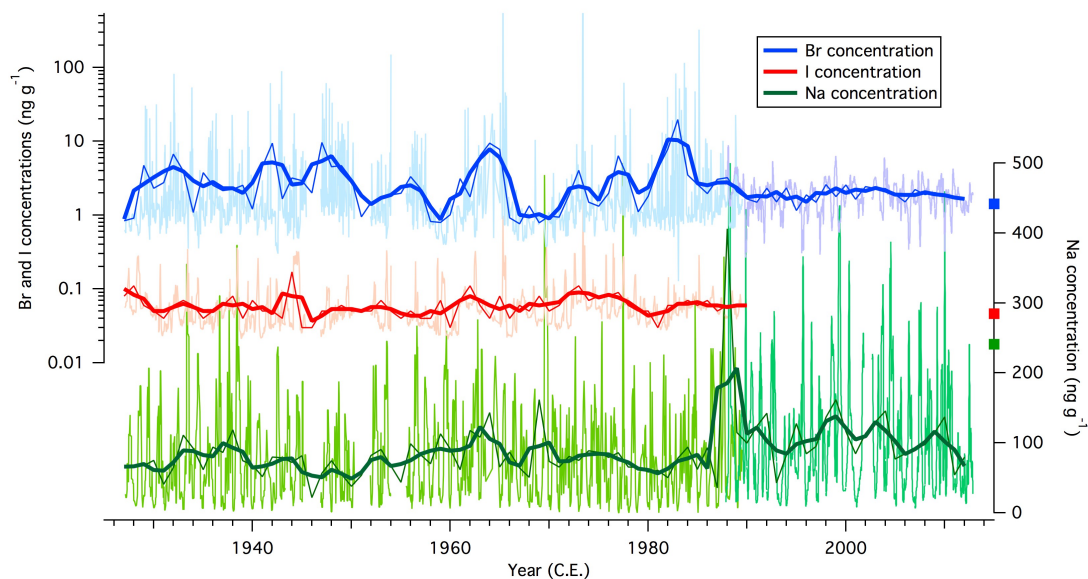
5 Figure 2: Antarctic sectors used for evaluating sea ice trends. Two sectors (90-110° E and 110-130° E) adjacent to Law Dome have been isolated and used to calculate past sea ice area. The image shows an example of sea ice cover for the month of May 2015 given as sea ice concentration (%) per grid cell.



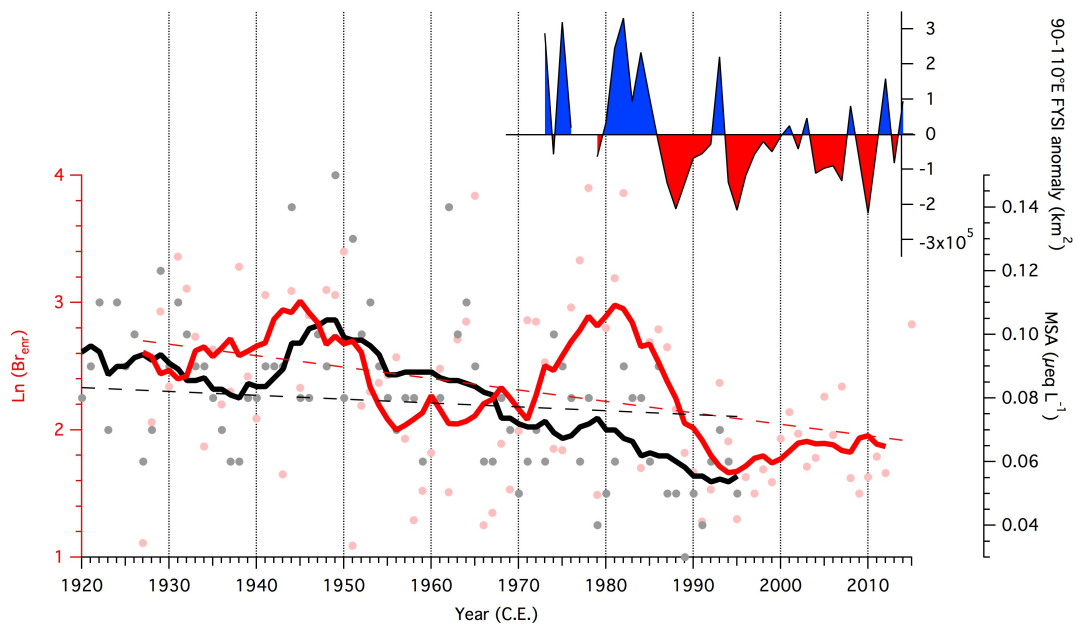
5

Figure 3: First year sea ice (FYSI) trends calculated from satellite microwave radiometer observations. The 90-110° E and 110-130° E trends shown here correspond to the two sectors indicated in Fig. 2. The 90-130° E FYSI data series (fuchsia) is the sum of the 90-110° E (red) and 110-130° E (green) data series. For comparison to previous studies, we include corresponding data series from Jo Jacka (Jacka, 1998) and NSIDC (Fetterer et al., 2002).

10



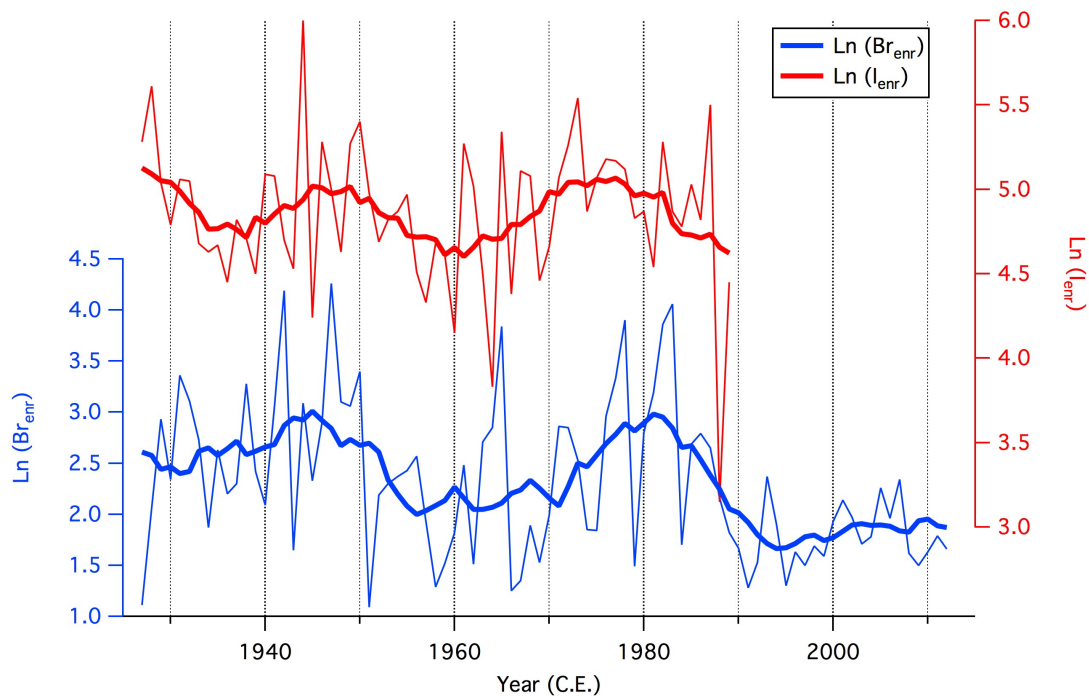
5 Figure 4: Time series of sodium, iodine and bromine concentrations at Law Dome. Raw data are shown in pale colours, with annual means shown by a thin line and three-year running means shown by a thick line. Different shades of blue and green are used to distinguish data from DSS0506 (1927-1989) and DSS1213 (1987-2013). The squares indicate average values from the DSS1516 snow pit.



5

Figure 5: Trends of bromine enrichment (Br_{enr} , red), MSA (black) and First Year Sea Ice (FYSI) at Law Dome. Bromine enrichment and MSA data are shown as annual averages (circles) as well as 11-year (thick lines) running means. Linear regression trends are shown as dotted lines. FYSI for the 90-110° E sector is shown as annual anomalies from the 1973-2014 average.

10



5 **Figure 6: Time series' of bromine and iodine enrichment beyond sea salt concentrations.** As described in Sect. 3.2, sea salt is represented by sodium. Bromine and iodine show similar trends, pointing to a common source representing variability in local sea ice extent.

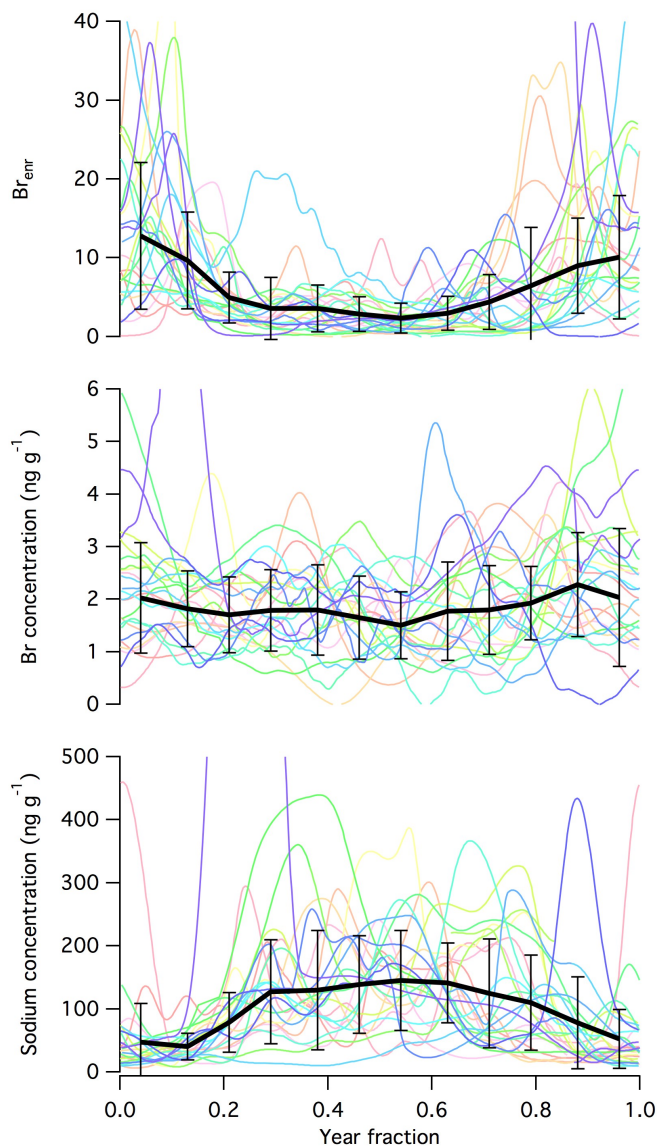


Figure 7: Seasonality of sodium and bromine concentrations and bromine enrichment (Br_{enr}) in the DSS1213 firn core. Each colour corresponds to one year of data with the same year represented by the same colour. The year fraction has been separated into 12 months, with 0.42 representing January and 0.96 representing December. The error bars show 1 standard deviation for the 26 years sampled.

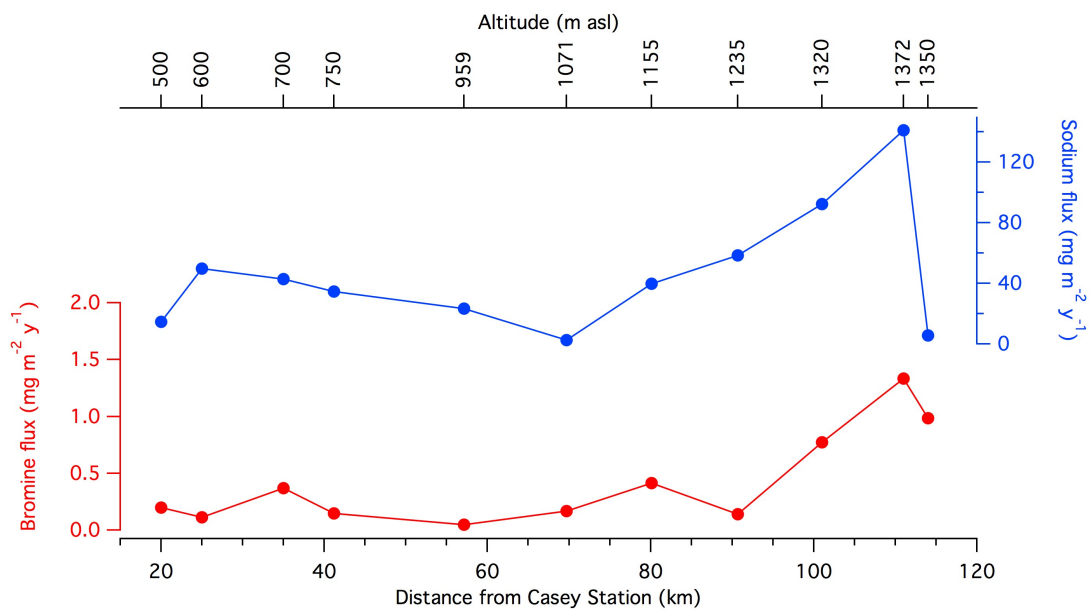


Figure 8: Fluxes of sodium and bromine along the 2016 Law Dome Traverse (indicated in Fig. 1).

5